Pure & Appl. Chem., Vol. 67, No. 6, pp. 1011–1018, 1995.
Printed in Great Britain.

Thermochemistry of fuel–clad and clad–coolant interactions of fast breeder reactors

C.K. Mathews

Chemical Group, Indira Gandhi Centre for Atomic Research,
Kalpakkam - 603 102, India

Abstract: In a fast breeder reactor, the stainless steel fuel clad is exposed to flowing sodium on the outside and the fuel on the inside. The chemical interaction of the clad with the fuel on the one hand, and with liquid sodium on the other, is discussed in this paper, in the light of experimental measurements carried out primarily in the author's laboratory. In the case of the mixed carbide fuel, the possibility of clad carburization is examined, while the role of fission product tellurium in the internal corrosion of the clad is the focus of attention in the discussion on the mixed oxide fuel. In oxygen-free sodium, clad corrosion depends on the solubility of the alloying elements in the coolant. When oxygen is present, the corrosion rate is enhanced, and this can be understood in terms of the thermochemistry of Na-M-O ternary systems, where M represents the constituents of the clad.

INTRODUCTION

In a fast breeder reactor, energy is produced in the core of the reactor by nuclear fission induced by fast neutrons. The high specific energy of the fast reactor fuels, the high temperature of operation and the hard neutron spectrum have led to the choice of liquid sodium as the coolant in these reactors. Thus liquid sodium transports the heat generated in the core to an intermediate heat exchanger (IHX) in a closed loop called the primary sodium loop. This heat is further transported from the IHX to steam generators by the sodium in a secondary heat transfer circuit. A mixed oxide of uranium and plutonium is the fuel used in most of the fast breeder reactors. However, there is considerable interest in developing advanced fuels which give superior performance in terms of fuel burn-up, linear rating and breeding gain. Carbides, nitrides and metallic alloys of uranium and plutonium [MC, MN and MZr when M = U + Pu] are receiving a good deal of attention in this respect on account of their high density and high thermal conductivity.
The Fast Breeder Test Reactor [FBTR] at Kalpakkam uses a mixed carbide of uranium and plutonium as the driver fuel. The fuel is normally made in the form of pellets, of about 5 mm diameter. A stack of such pellets is sealed in a cladding tube to make a fuel pin. A fuel subassembly contains a number of such pins. The thin-walled cladding tube is made of 316 stainless steel or its stabilized varieties. It is subjected to chemical interaction from the outside by liquid sodium and from the inside by the fuel. In addition, the expansion of the fuel due to processes such as fuel swelling brings the clad under mechanical stress. Any wastage of the clad through corrosion on the inside or on the outside reduces its strength and hence is a potential cause for fuel failure. This paper deals with the thermochemistry of fuel-clad and clad-coolant interactions.

FUEL-CLAD COMPATIBILITY IN THE CARBIDE FUEL

The mixed carbide fuel

The Fast Breeder Test Reactor (FBTR) in the Indira Gandhi Centre for Atomic Research, Kalpakkam, presently employs a mixed carbide with a Pu/(U+Pu) ratio of 0.7 as fuel. The cladding material is ss 316. Carburization of the clad is one of the principal concerns while using the mixed carbide fuel. There are two modes by which stainless steel clad can be carburized. In the first mode, transport of carbon to and from the clad could occur at the interface between the fuel and the clad, depending upon the difference in the carbon potential between them. In the second mode, carburization is brought about by the pressure gradient of CO(g) prevailing within the fuel pin. In order to maintain satisfactory mechanical properties, stainless steel has to contain an optimum amount of carbon. Hence any change in carbon content resulting from carbon transport could have a detrimental effect on the mechanical integrity of the steel.

Carbon potential

The carbide fuel consists mainly of the monocarbide (U,Pu)C with a small admixture of the sesquicarbide phase. Oxygen and nitrogen are unavoidable impurities which dissolve in the monocarbide phase. Thus we have a multicomponent system of U-Pu-C-N-O to consider. In order to assess the possibility of clad carburisation, we must have data on the carbon potential of the fuel and the clad. Carbon potential of stainless steel has been measured by many investigators (1-5). In our laboratory we have measured the carbon potentials of the fuel with Pu/(U+Pu) ratios of 0.55 and 0.70 in the temperature range of 973 to 1173 K by using a methane-hydrogen gas equilibration technique. We have also measured the carbon activity of the mixed carbide with a Pu/(U+Pu) ratio of 0.7 over the temperature range 847 to 913 K by employing an electrochemical carbon meter. Garg et al (6) measured the carbon potential of the carbide fuel of Pu/(U+Pu) = 0.7 over the temperature range 1273 to 1373 K by using an isopiestic technique. The measured carbon potentials for the mixed carbides with Pu/(U+Pu) ratios of 0.70 and 0.55 are shown in Fig. 1. The samples consisted mainly of the monocarbide phase with an 8% admixture of the sesqui-carbide phase. The oxygen content was 3900 and 3640 wppm and the nitrogen content was 728 and 835 wppm respectively.

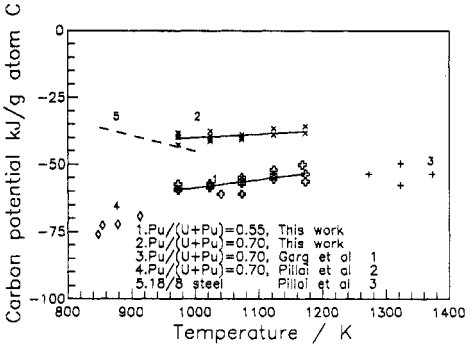

Fig.1 CARBON POTENTIAL OF MIXED CARBIDE FUELS

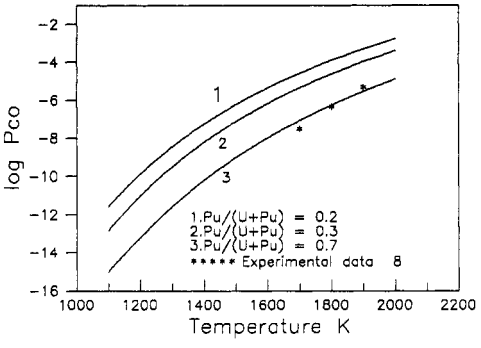

Fig.2 Pco OVER MIXED CARBIDE FUELS

Sayi et al. (7) measured the equilibrium CO pressures over FBTR fuel (Pu/(U+Pu) = 0.70) in the temperature range of 1700 to 1930 K. No other data on the equilibrium CO pressures of mixed carbides are available in the literature. Hence we computed the equilibrium CO pressures by employing an ideal solution model for various solid solutions in the U-Pu-C-O-N system. The equilibrium partial pressures of CO,Pu and N_2 as well as the carbon potential of the mixed carbide fuel were calculated, in our laboratory, as a function of Pu content, impurity (O,N) concentration, sesquicarbide content and temperature (9). Two different calculational methods were used - one based on a set of equilibrium relations between the co-existing phases and the other based on free energy minimisation employing the computer programme SOLGASMIX-PV. Typical results are given graphically in Fig. 2, which shows the variation of p_{CO} as a function of temperature.

Clad carburization

The carbon potential of 18/8 stainless steel at 950 K is approximately -40 kJ mol^{-1} (3). A comparison of the carbon potential of the mixed carbide (Pu/(U+Pu) = 0.7) with that of the stainless steel clad tube (Fig.1), reveals that the steel cannot be carburized by the carbide fuel under isothermal thermodynamic equilibrium conditions. The carbon potential of the carbide fuel with a Pu/(U+Pu) ratio of 0.55 is comparable with that of the stainless steel clad; hence the driving force for carbon transport, under isothermal conditions, is small. However, under the prevailing temperature gradient in the fuel pin there is a possibility of clad carburization in spite of the lower carbon potential of the fuel. This can be explained by considering the following equilibrium reactions:

At the fuel-surface (temperature T_1): $[C]_{fuel} + (CO_2) = 2\,(CO)$ (1)

At the clad-surface (temperature T_2): $2\,(CO) = [C]_{clad} + (CO_2)$ (2)

If a constant pressure ratio of p^2_{CO}/p_{CO2} is assumed throughout the fuel pin, it can be shown by thermodynamic analysis [8] that the CO/CO_2 gas mixture in equilibrium with the fuel at higher temperature will carburize the clad in spite of the lower carbon potential of the fuel. Kinetic factors will also be important in determining the degree of carburization.

It has been reported [10-11] that the carburization of the clad (by the transport of carbon via CO gas) becomes noticeable only when p_{CO} is more than 10^{-4} MPa. (fuel-centre temperature: 1600 to 1900K; fuel-surface temperature: 1100 to 1550 K; clad temperature: 900K). From Fig.2, it is clear that even at 1900 K the p_{CO} in the present FBTR fuel is $< 10^{-6}$ MPa. Hence there is no possibility of carburization of the clad by the mixed carbide fuel with a Pu/(U+Pu) ratio of 0.7. It is also clear from the figure that the p_{CO} of the mixed carbide fuel decreases with increasing plutonium content. Hence mixed carbide fuels with high plutonium contents

[Pu/(U+Pu) > 0.5] may not carburize the clad by gas phase carbon transport mechanism. For fuels with low plutonium content, the oxygen level must be brought down to low values to minimise carburization. The oxygen concentration specified for such fuels is <500 wppm.

INTERNAL CORROSION OF THE CLAD IN THE MIXED OXIDE FUEL

The mixed oxide fuel

The mixed oxide fuel of uranium and plutonium is quite compatible with the stainless steel clad. This single phase fuel, which is fabricated in the hyperstoichiometric state does not oxidise the clad. However, internal corrosion has been observed at high burn-up (>5 at.%). Fission products are expected to play a role in the chemical attack on the clad and indeed fission products Cs, I, and Te have observed in the reaction zone. Initially it was thought that iodine would be the culprit. However, the low yield of this element in fission and the high stability CsI makes its role in the corrosion process to be less probable than that of the more abundant tellurium.

Thermochemistry of metal-tellurium systems

In order to assess the role of tellurium in clad corrosion, reliable thermodynamic data and phase relationships in M-Te binary systems (M=component of the clad) are required. In our laboratory we have investigated the binary systems of tellurium with Fe, Cr, Ni, Mo and Mn and used this data to examine the possible mechanism for the internal corrosion of the clad (12-21). The principal technique used in this study was high temperature mass spectrometry. The experimental details, the derivation of partial pressures from the measured data and the method of determining phase boundary compositions are reported elsewhere (12-22).

$Te_2(g)$ and Te(g) were the tellurium bearing species observed in most of the tellurides. Mn(g) was observed in the case of Mn+MnTe phase field. Plots of log(p) vs 1/T for $Te_2(g)$ for the various M-MTe biphasic mixtures studied are shown in Fig. 3. At a particular temperature, the lowest $Te_2(g)$ partial pressure is seen in case of Cr-$CrTe_x$. The boundary compositions of the telluride phases coexisting with the metal, were also deduced from weight loss experiments.

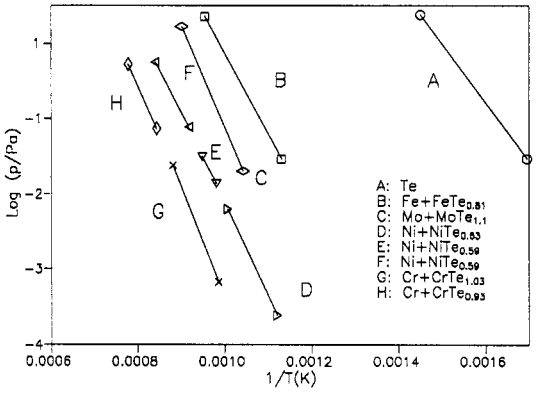

Fig.3 Log $p(Te_2)$ Vs 1/T for M-MTe_x phase fields

TABLE 1. Enthalpy and Gibbs energy of formation (kJ/mol) of binary MTe_x phases of relevance to fuel-clad interaction

Phase	T(K)	Reference state	$\Delta_f H_m^o$	$\Delta_f G_m^o$
$FeTe_{0.81}$	298.15	Fe(s),Te(s)	-17.2	-21.1
$FeTe_{0.94}$	298.15	Fe(s),Te(s)	-27.8	-29.7
$NiTe_{0.63}$	298.15	Ni(s),Te(s)	-33.3	-35.0
$NiTe_{0.59}$	1038.15	Ni(s),Te(l)	-27.7	-30.1
$NiTe_{0.59}$	1140.00	Ni(s),Te(l)	-30.5	-30.7
$CrTe_{1.03}$	298.15	Cr(s),Te(s)	-70.8	-73.0
$CrTe_{1.03}$	1076.50	Cr(s),Te(l)	-91.5	-63.5
$CrTe_{1.03}$	1232.50	Cr(s),Te(l)	-67.6	-55.7
$MoTe_{1.10}$	298.15	Mo(s),Te(s)	-66.4	-65.1
$MoTe_{1.10}$	950.00	Mo(s),Te(l)	-63.7	-48.4
$MoTe_{1.30}$	950.00	Mo(s),Te(l)	-67.0	-54.6
$MnTe_{0.80}$	298.15	Mn(s),Te(s)	-86.8	-90.0

The vapour pressure vs temperature relations obtained over various phase fields and the boundary compositions (mostly determined by us) were used to obtain the reaction enthalpies for vaporisation reactions such as

$$<MTe_x> = <MTe_y> + [(x - y) / i]\ (Te_i) \quad (3)$$

(values of x and y depends on the phases involved; y=0 for metal and i=1,2,3), by using the second - as well as the third law methods.

Combining the above reaction with the reaction

$$2<Te> = (Te_2) \quad (4)$$

it is possible to derive the enthalpies and free energies of formation of the MTe_x phases. The required data for reaction (4) were also determined by us (21). The details of the results are given in Table 1.

Role of tellurium in clad corrosion

In the fuel-clad gap, tellurium is associated with liquid cesium which deoxidises the inner surface of the clad. Thus the reaction between tellurium and the constituents of stainless steel to form appropriate metal tellurides can be represented as:

$$[M]_{ss} + x\{Te\} = <MTe_x> \quad (5)$$

where M refers to alloying constituent of stainless steel. The threshold tellurium potential for the above reaction is given by the following expression (23):

$$\Delta\bar{G}_{Te} = RT\ (\ln a_{Te} - (1/x)\ \ln a_M) \quad (6)$$

where a_{Te} is the activity of tellurium and a_M is the activity of M in stainless steel. In terms of partial pressure of $Te_2(g)$, the above equation can be rewritten as follows

$$\Delta\bar{G}_{Te} = RT\ [(1/2)\ \ln (p(Te_2)/p^\circ(Te_2)) - (1/x)\ \ln a_M] \quad (7)$$

We have determined the partial pressures of tellurium ($p(Te_2)$) for each of the M-MTe_x binary phase fields, as well as compositions (x). Taking the reported pressures over pure tellurium ($p^\circ(Te_2)$) from Gronvold et al. (24) and a_M values from Azad et al.(25), the threshold tellurium potential for the formation of the metal tellurides of interest can be readily calculated. The results are given in Fig. 4.

The tellurium potential prevalent in the fuel-clad gap depends on the availability of Cs to tie down tellurium. In a mixed-oxide fuel pin, Cs can form ternary oxides such as Cs_2MO_4 (M=U+Pu), Cs_xCrO_4 and Cs_2MoO_4. This would decrease the availability of Cs and thus increase the tellurium potential. Adamson et al. (26) proposed that the most probable reaction that controls tellurium potential in the fuel-clad gap as:

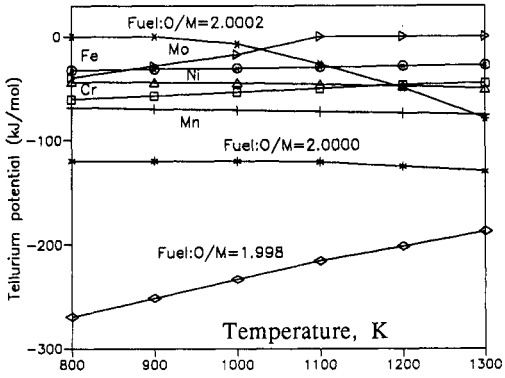

Fig. 4 Tellurium potential for various equilibria. In the fuel-clad gap: Cs_2Te | $MO_{2\pm x}$ | Cs_2MO_4, where $M=U_{0.75}Pu_{0.25}$ &O/M=1.9998, 2.0000 and 2.0002. At the clad: $[M]_{ss}$ | MTe_x, where M=Fe, Ni, Cr, Mo and Mn. For x values see Table 1.

$$[Cs_2Te]_{melt} + <MO_{2\pm x}> + ((2\pm x)/2)\ (O_2) = <Cs_2MO_4> + [Te]_{melt} \quad (8)$$

This leads to the following expression for Te potential:

$$\Delta\bar{G}_{Te} = (\Delta_fG^\circ) + RT\ \ln a_{Cs2\ Te} + ((2\pm x)/2)\ RT\ \ln (p_{O2}) \quad (9)$$

where $(\Delta_fG^\circ) = (\Delta_fG^\circ)_{<UO_2>} + (\Delta_fG^\circ)_{<Cs_2Te>} - (\Delta_fG^\circ)_{<Cs_2UO_4>} - (\Delta_fG^\circ)_{\{Te\}}$.

In deriving the above expression, it is assumed that $MO_{2\pm x}(s)$ and $Cs_2MO_4(s)$ phases have the same Pu/U ratio and that a solution between Cs_2Te and Te can exist in the melt.

Tellurium potentials have been computed for the mixed oxide fuel with a composition $M= U_{.75}Pu_{.25}$and three different O/M ratios near stoichiometric value. The oxygen potentials were calculated by using the models developed by Krishnaiah and Sriramamurti (27). The necessary thermodynamic data for Te(s,l) (24), $UO_2(s)$ (26), $Cs_2Te(s)$ (28,29) and $Cs_2UO_4(s)$ (30) were taken from the literature. The results are also plotted in Fig. 4. The temperature range is so chosen as to represent that of the fuel-clad gap under different operating conditions. Whenever the calculated tellurium potential for reactions (5) and (8) yielded a positive value we have equated it to zero. Such a positive value is an indication that the equilibria represented by equations (4) and (7) are no more valid under such conditions.

An examination of Fig. 4 shows that the tellurium potential prevailing in the fuel clad gap is insufficient for clad attack when the O/M is stoichiometric or below. However, clad corrosion is possible with hyper-stoichiometric fuel. The first telluride that is likely to be formed is that of Mn. Since the fuel is unlikely to be hyper- stoichiometric in a fast breeder reactor, the above analysis suggests that tellurium may not be responsible for clad corrosion under equilibrium conditions. The situation in mixed carbide or mixed nitride fuel is more benign, as Cs availability in the fuel-clad gap is likely to be higher, thereby depressing the tellurium potential.

It must, however, be recognised that the above analysis is based on equilibrium thermodynamics and does not take into account the effect of radiation. It has been proposed (31-33) that fission fragments can produce energetic helium atoms and ions, through knock-on processes, and these in turn can cause the dissociation of CsI(g), thus increasing the iodine potential in the fuel-clad gap. It would be worthwhile generating supporting experimental data for such an increase of I or Te potential. So far, even in case of iodides only experiments involving electron irradiation have been reported, but none involving fission fragments and helium, which is the bond gas in the fuel pin.

CLAD-COOLANT INTERACTIONS

Liquid sodium, which is used as the coolant in the fast breeder reactor, is quite compatible, in the pure state, with the austenitic and ferritic steel structural materials (34). However, traces of impurities play an important role in the corrosion, mass transport and other processes taking place in the heat transport loops of the reactor. Even parts per million (wppm) levels of oxygen causes corrosion in the high temperature sections of the loop and the corrosion products get transported through the liquid sodium medium to cooler parts. Some of these corrosion products and fission products which find their way into sodium can cause high radiation levels when they deposit on parts like heat exchangers and pumps which have to be periodically maintained. Thus one must not only control and monitor the oxygen impurity level, but also understand the transport and deposition of radionuclides in the reactor. Thermochemistry of the ternary Na-M-O systems, where M stands for the components of the structural materials, figure prominently in any analysis of the corrosion of fuel cladding in flowing sodium.

Corrosion in low-oxygen sodium

In pure sodium containing low levels of oxygen (a few wppm or less), the corrosion rate is low and this proceeds by the selective leaching of alloying elements (35). The presence of temperature gradients in the heat transport circuits enhances this process. For understanding of this phenomenon, data on the solubility of the various alloying elements in sodium are required. While the solubility of some of these were available in the literature, those of Mn and Mo in oxygen-gettered liquid sodium was measured in our laboratory using an equilibration technique (36) to obtain the following expressions:

$$\log S \text{ (wppm Mn)} = 3.6406 - (2601.7/T) \quad [T = 550 - 811 \text{ K}] \tag{10}$$

$$\log S \text{ (wppm Mo)} = 2.7380 - (2200/T) \quad [T = 500 - 720 \text{ K}] \tag{11}$$

Figure 5 gives the solubilities of the alloying elements in sodium as a function of temperature. Because of their higher solubilities, nickel and manganese are preferentially leached out from the steel under low oxygen conditions. The loss of alloying elements makes the γ-phase unstable and the depleted layer of the austenitic material transforms to ferrite (37). In fast flowing sodium the kinetics of selective leaching process gets controlled by the diffusion of alloying elements in the steel matrix to the corroding surface.

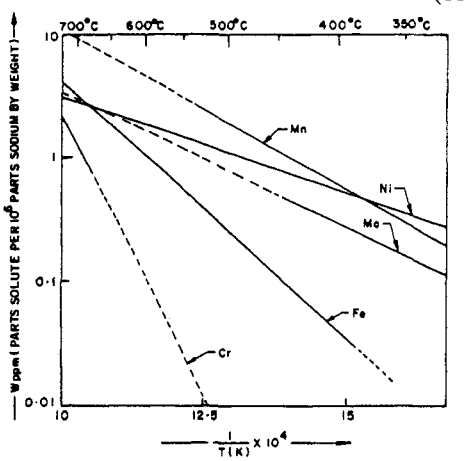

Fig. 5 Solubilities of Fe, Cr, Mo, Mn and Ni in sodium

Effect of dissolved oxygen

The corrosion rate of structural materials is enhanced by an increase in the oxygen concentration in sodium. The corrosion rate of stainless steel in fast flowing sodium is dependent on n th power of oxygen concentration. was reported by Thorley and Tyzack reported the value of n as 1.5 (38). This strong dependence of corrosion rate on oxygen concentration indicates a chemical reaction involving oxygen, leading to a ternary oxide formation. This reaction would be related to the stability of the oxides of the alloying elements in liquid sodium. If the oxide of the alloying element is less stable than Na_2O, then it would be reduced to the metal by sodium. If the oxide is stabler than Na_2O, then the metal is readily oxidised by sodium. If the oxide is of comparable stability, ternary oxides of sodium and the alloying element are likely to be formed. The alloying elements Fe, Cr, Ni, Mn and Mo generally fall in the last category. Among these, the oxides of Fe, Ni and Mo are less stable and hence form ternary oxides of lower stability than those of Cr and Mn.

The literature data on the ternary Na-M-O (M = Fe, Cr, Ni, Mn, Mo) systems was far from complete when the studies were taken up in our laboratory. Ternary oxides formed in the case of each of the allying elements were reported but their relative stabilities were not unequivocally established. Except in the case of Na-Cr-O system, thermodynamic data for the ternary oxides and the equilibrium phase diagrams were also not available. We have carried out detailed investigation in these ternary systems with a view to bringing out the chemical aspects of the mass transfer in liquid sodium circuits.

Na-Cr-O system

Under the normal operating conditions of a sodium-steel circuit, the ternary compound that is observed is $NaCrO_2$. Threshold oxygen level above which this compound would form is an important parameter. This can be obtained by measuring the oxygen potential in Na-$[Cr]_{ss}$-$NaCrO_2$ phase field or can be deduced from the free

energy of formation of $NaCrO_2$. Values reported in literature from these two approaches were quite different. In view of this both were remeasured in our laboratory (39). The discrepancy between the two sets of data were established to be due to the interaction of dissolved carbon with chromium during in-sodium investigations. Carbides of chromium are very stable and they participate in the equilibrium leading to the formation of $NaCrO_2$(s). Taking this phenomenon into account, a phase stability diagram of the Na-Cr-O-C system was constructed. This diagram, shown in Fig. 6, explains the following observations in sodium loops reported in the literature: (1) only chromium carbide deposits are noticed in sodium loops when oxygen level is low (40); (2) threshold oxygen levels for $NaCrO_2$ formation directly measured in sodium are higher than those computed by considering only the Na-Cr-O system.

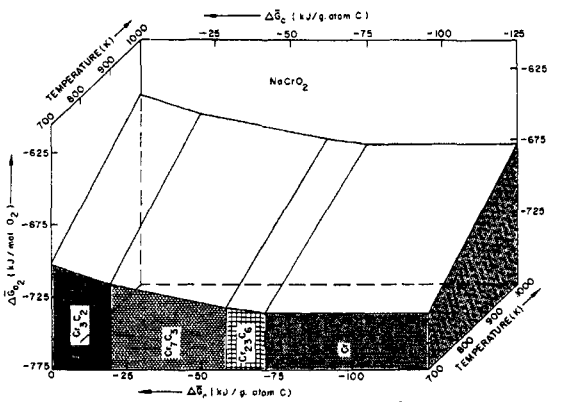

Fig. 6 Phase stability diagram of Na-Cr-O-C system.

Na-Mo-O system

The ternary Na-Mo-O system was recently investigated in our laboratory (41,42). By employing various experimental techniques, it was established that up to 681 K only Na_2O exists in equilibrium with the metallic phases. Above this temperature Na_4MoO_5 is the equilibrium phase. Phase relationships between other ternary oxides in this system were also established and the phase diagram of this system was deduced. The equilibrium oxygen potential in the Na-Mo-Na_4MoO_5 phase field was also measured and the Gibbs free energy of formation Na_4MoO_5 was derived from this data (41). The threshold oxygen concentration for the formation of Na_4MoO_5 in sodium systems, based on this Gibbs energy of formation, are 843 ppm at 700 K and 974 ppm at 800 K. Under normal operating conditions of a sodium circuit, when oxygen levels are much lower, only metallic dissolution process is possible. Considering the solubility of Mo in sodium and its activity in stainless steel, significant leaching would not take place.

Na-Fe-O system

Iron is the major component of steels and the bulk corrosion of steels in sodium systems is essentially the loss of iron through oxidation. However, thermodynamic data available in the literature suggests that a ternary oxide is likely to be formed only at high oxygen levels (>1000 ppm). This is contrary to the experience on corrosion in sodium systems. Enhancement of corrosion occurs at much lower oxygen levels. Therefore, a detailed investigation of this system was carried out in our laboratory.

Experiments involving equilibration of iron oxides with liquid sodium, pseudo-isopiestic equilibration of binary and ternary oxides with sodium vapour and solid state reactions of oxides of iron and sodium were carried out. The experimental results have shown that up to a temperature of 623 K it was found that liquid sodium co-exists with Fe(s) and Na_2O(s). Oxygen potential measurements carried out in liquid sodium equilibrated with oxides of iron clearly indicated the appearance of a ternary oxide at temperatures above 623 K (43). Results of isopiestic equilibration experiments and solid state equilibrations have shown that Na_4FeO_3 coexists with metallic iron and liquid sodium at 923 K. Differential thermal analysis of liquid sodium samples equilibrated with iron oxides showed a reversible transition at 760 ± 6K. Similar observations were made by Charles et al during their studies in Na-Fe-O system [44]. We had attributed this to the appearance of another ternary oxide phase in liquid sodium [45] and similar conclusions were made by Bhat et al based on their oxygen potential measurements in sodium using a solid electrolyte technique [46]. With a view to identifying the nature of reactions leading to the formation of ternary oxides, differential scanning calorimetric measurements with varying ratios of oxides of iron and sodium as well as mixtures of Na_4FeO_3 and sodium were carried out. These results coupled with identifications of the products of solid state reactions between Na_2O(s) and FeO(s) have shown that the reversible transition occurring at 760K is the appearance of a liquid phase of Na_4FeO_3. Na_4FeO_3 co-exists with metallic iron and sodium above 623 K. From the measured oxygen potential data, Gibbs energy of formation of Na_4FeO_3 could be derived and is given below.

$$\Delta_f G^\circ_{<Na_4FeO_3>} \text{ (J mol}^{-1}\text{)} = -1168881.3 + 271.44\ T\ (K) \qquad (12)$$

Phase fields not involving liquid sodium were also established by solid state equilibrations. Based on these data isothermal cross sections of Na-Fe-O system have been derived. Figure 7 shows the isothermal cross section at 760 > T > 623 K.

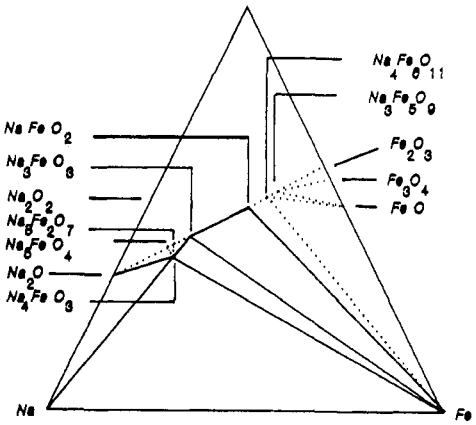

Fig. 7 Phase diagram of Na-Fe-O system [760 > T > 623 K]

Na-Ni-O system

Corrosion data in the literature have shown that nickel corrosion in sodium is not enhanced by oxygen content in sodium. $NaNiO_2$ and Na_2NiO_2 are the reported ternary compounds, although their thermodynamic properties and phase diagram of Na-Ni-O system were not available. A detailed investigation was undertaken to elucidate the phase relationships in this system in our laboratory [47] and the equilibrium phase diagram of was established. The results have shown that no ternary oxide of nickel is stable towards liquid sodium, and hence corrosion of nickel would be expected to be independent of oxygen in sodium.

Threshold oxygen concentrations for ternary oxide formation in Sodium-stainless steel-oxygen system

The enhancement of the corrosion of the structural steels by dissolved oxygen proceeds by the formation of ternary compounds according to the following general equilibrium:

$$\{Na\} + x\,[M]_{ss} + y\,[O]_{Na} = <NaM_xO_y> \quad (13)$$

The threshold oxygen potentials for the formation of the ternary oxides that can coexist with liquid sodium were calculated and are shown in Fig. 8. Effect of carbon would be to raise the threshold oxygen potentials, when the alloying elements form stable carbides. Cr, Mo, and Mn fall in this category. It can be seen that only $NaCrO_2$ is expected to be formed in operating sodium systems where oxygen levels are not expected to be above 10-15 ppm.

It is also seen that Na_4FeO_3, which is of relevance to explain the bulk corrosion process, would be formed at temperatures above 640K and at oxygen concentrations above 275 ppm. To explain the enhancement of steel corrosion in oxygen contaminated sodium, Weeks and Isaacs have proposed a model for corrosion of steels which involved the dissolution of a solvated complex involving iron and oxygen (48). Assuming that Na_4FeO_3 is present as dissolved species, attempts were made to calculate the enhanced iron solubility for various dissolved oxygen concentrations by considering the following equilibrium:

$$3\,[Na_2O]_{Na} + <Fe> = [Na_4FeO_3]_{Na} + 2\{Na\} \quad (14)$$

$$k = a_{Na_4FeO_3} * [a_{Na_2O}]^{-3} \quad (15)$$

The equilibrium constant, k, at a given temperature (above 623 K) was calculated by using the Gibbs energy of formation of Na_4FeO_3(s) from the present work and that of Na_2O(s) from ref.49. For a known oxygen level in sodium, which fixes the activity of Na_2O, the activity of the ternary compound was computed. By using the estimated solubility of the ternary compound in sodium by Thompson (50), the concentration of the dissolved ternary was obtained, assuming Henry's law valid for this dissolution. The results indicated negligible enhancement of solubility implying,perhaps, the non-validity of the Henry's law for the dissolution process. This is not unexpected because of the high interaction that exists in the Na-Fe-O system.

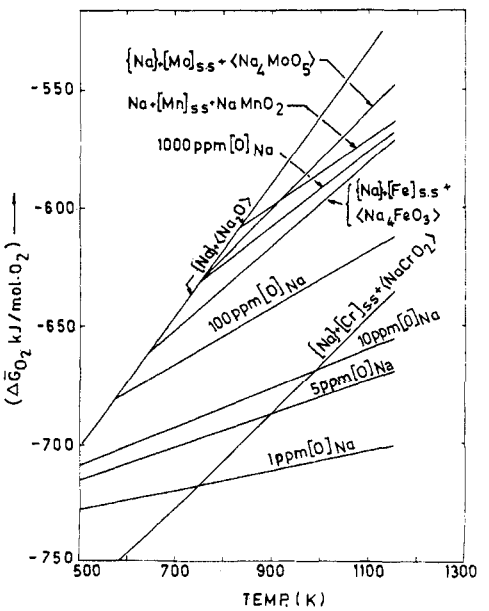

Fig. 8 Oxygen potentials for Na-$[M]_{ss}$-NaM_xO_y and Na-Na_2O systems

REFERENCES

1. K. Natesan and T.F. Kassner. Metall.Trans. **4**, 2557 (1973).
2. V.H. Tuma et al. Archiv.Eisenhuttenw. **9**, 727 (1969).
3. S.R. Pillai and C.K. Mathews. J. Nucl. Mater. **150**, 31 (1987).
4. M.Handa et al. J. Nucl. Mater. **116**, 178 (1983).

5. G.L. Goswami et al, Proc. Seminar on Fast Reactor Fuel Cycle, IGCAR, Kalpakkam, India, Feb. Vol.II, p.45, (1986).
6. S.P. Garg et al, ibid, Vol.II, p.61.
7. Y. Sayi et al. ibid, Vol.II, p.63.
8. S.P. Garg et al. ibid, Vol.II, p.56.
9. M. Sai Baba et al. J. Nucl. Mater. **144**, 56 (1987).
10. J.M. Horspool et al. Proc. Fuel and Fuel Elements for Fast Reactors, Vol.1, p.3, IAEA, Vienna (1974).
11. M.G. Adamson, UKAEA report, AERE-R-6897.
12. B. Saha et al. J. Nucl. Mater. **130**, 316 (1985).
13. M. Sai Baba et al. J. Chem. Thermodyn. **20**, 1157 (1988).
14. R. Viswanathan et al. J. Nucl. Mater. **149**, 302 (1987).
15. R. Viswanathan et al. J. Nucl. Mater. **167**, 94 (1989).
16. R. Viswanathan et al. International Symposium on Calorimetry and Chemical Thermodynamics, Moscow, USSR, June 1991.
17. R. Viswanathan, Ph D thesis, Madras University, October 1991.
18. R. Viswanathan et al. J. Chem. Thermodyn. **21**, 1183 (1989).
19. R. Viswanathan et al. J. Chem. Thermodyn. **25**, 533 (1993)
20. M. Sai Baba et al. Paper presented at the 12th IUPAC conference on Chemical Thermodynamics, Snowbird, Utah, August 16-21,1992.
21. M. Sai Baba et al. J. Nucl. Mater. **201**, 147 (1993).
22. C.K. Mathews, J.Nucl.Mater. **201**, 99 (1993)
23. B. Saha et al. High Temp.- High Pr. **20**, 47-58 (1988).
24. F. Gronvold, J. Drowart and E.F. Westrum, Jr, The Chemical Thermodynamics of Actinide Elements and Compounds, Part 4: The Actinide Chalcogenides (Excluding oxides) (IAEA,Vienna,1984)
25. A.M. Azad et al. J. Nucl. Mater. **144**, 94 (1987).
26. M.G. Adamson et al. J. Nucl. Mater. **130**, 375 (1985).
27. M.V. Krishnaiah and P. Sriramamurthy, J. Am. Ceram. Soc. **67**, 568 (1984)
28. E.H.P. Cordfunke and W. Ouweltjes,J. Chem. Thermodyn. **19**, 293 (1987)
29. E.H.P. Cordfunke et al. J. Chem. Thermodyn. **19**, 377 (1987)
30. E.H.P. Cordfunke ,J. Chem. Thermodyn. **18**, 503 (1986)
31. K.Konashi et al. J.Nucl. Mater. **116**, 86 (1983).
32. K.Konashi et al. J. Nucl.Mater. **125**, 244 (1984).
33. P.E. Potter, "Thermochemistry and Chemical Processing", Ed. C.K. Mathews, Indian Institute of Metals, Kalpakkam, 1991, 107-129.
34. H.U.Borgstedt and C.K.Mathews, Applied Chemistry of Alkali Metals,Plenum Press,New York(1987).
35. A.W.Thorley, Liquid Metal Engineering and Technology,BNES,London,vol.3,p.31(1984).
36. G.Periaswami, V.Ganesan, S.Rajan Babu and C.K.Mathews,in Material Behaviour and Physical Chemistry in Liquid Metal Systems (ed.)H.U.Borgstedt,p.411,Plenum Press,New York(1982).
37. H.U.Borgstedt, Rev.Coating and Corros.,**2**, 121(1977)
38. A.W.Thorley and C.Tyzack,in Liquid Alkali Metals,BNES,London,p.257(1973).
39. T.Gnanasekaran and C.K.Mathews, J.Nucl.Mater.**140**, 202(1986).
40. B.W.Kolster, J.Nucl.Mater.**55**, 155(1975).
41. T.Gnanasekaran et al. J.Nucl.Mater.**150**, 113(1987).
42. T.Gnanasekaran et al. J.Nucl.Mater.**165**, 210(1989).
43. R.Sridharan et al. J.Nucl.Mater.**167**, 265(1989).
44. R.G.Charles, Trans.Am.Nuclear Soc.**19**, 107(1974).
45. R.Sridharan et al.J.Alloys and Comp.**191**, 9(1973).
46. N.P.Bhat and H.U.Borgstedt,J.Nucl.Mater.**158**, 7(1988).
47. V.Ganesan, Ph.D. Thesis, University of Madras (1989).
48. J.R.Weeks and H.S.Isaacs,in Advances in Corrosion Science and Technology(eds)M.G.Fontana and R.W.Stachle,Plenum Press,New York, vol.3,p.1(1973).
49. D.R.Fredrickson and M.G.Chasanov, J.Chem.Thermodyn. **5** , 485 (1973).
50. R.Thompson, UKAEA Report AERE-9172 (1979).